

Surface-enhanced Raman scattering of molecules adsorbed on nanocrystalline Au and Ag films formed at the organic...

Mostafa El-Sayed


Chemical Physics Letters

Cite this paper

Downloaded from [Academia.edu](#) 

[Get the citation in MLA, APA, or Chicago styles](#)

Related papers

[Download a PDF Pack](#) of the best related papers 



[Low Cost, Ultra-Thin Films Of Reduced Graphene Oxide-Ag Nanoparticle Hybrids As SERS Bas...](#)

Neena John

[A review on the fabrication of substrates for surface enhanced Raman spectroscopy and their applic...](#)

Meikun Fan

[Two-step fabrication of nanoporous copper films with tunable morphology for SERS application](#)

xx xiao



Contents lists available at ScienceDirect

Chemical Physics Letters

journal homepage: www.elsevier.com/locate/cplett

Surface-enhanced Raman scattering of molecules adsorbed on nanocrystalline Au and Ag films formed at the organic–aqueous interface

Barun Das^{a,b}, Urmimla Maitra^{a,c}, Kanishka Biswas^{a,b}, Neenu Varghese^a, C.N.R. Rao^{a,b,c,*}

^aChemistry and Physics of Materials Unit, New Chemistry Unit, and CSIR Centre of Excellence in Chemistry, Jawaharlal Nehru Centre for Advanced Scientific Research, Jakkur P.O., Bangalore 560 064, India

^bSolid State and Structural Chemistry Unit, Indian Institute of Science, Bangalore 560 012, India

^cInternational Centre for Materials Science, Jawaharlal Nehru Centre for Advanced Scientific Research, Jakkur P.O., Bangalore 560 064, India

ARTICLE INFO

Article history:

Received 2 June 2009

In final form 22 June 2009

Available online 25 June 2009

ABSTRACT

Surface-enhanced Raman scattering (SERS) of pyridine adsorbed on ultrathin nanocrystalline Au and Ag films generated at the liquid–liquid interface has been investigated. The shifts and intensification of bands formed with these films comprising metal nanoparticles are comparable to those found with other types of Au and Ag substrates. SERS of rhodamine 6G adsorbed on Ag films has also been studied. The results demonstrate that nanocrystalline metal films prepared by the simple method involving the organic–aqueous interface can be used effectively for SERS investigations.

© 2009 Elsevier B.V. All rights reserved.

1. Introduction

Since the first observation by Fleischmann et al. [1] in 1974, surface-enhanced Raman scattering (SERS) has been employed extensively as an important tool for molecular detection. Because of the enhanced vibrational signals, low detection limits, and good adsorbate selectivity, SERS has a good potential for applications in various areas. Surface roughness, particle size and shape, the nature of the analyte and the wave length of laser excitation are the important factors that determine the magnitude of surface enhancement [2–7]. The two major enhancement mechanisms are the electromagnetic (EM) enhancement associated with the large local fields caused by surface plasmon resonance and the chemical enhancement caused by chemical interaction between the molecule and the metal surface. In noble metals, EM enhancement plays a dominant role. In early studies on SERS, roughened Au and Ag surfaces were used as substrates. SERS studies based on Ag [1,8–15], Au [8,9,16–19] and other metals such as Pt, Ru, Rh, Pd, Fe, Co and Ni [20–25] as well as the metallic oxide ReO_3 [26] have been reported. Since wider applications of SERS depend on the development of highly enhancing substrates, there have been efforts to develop improved substrates for enhancement. Thus, Yan and co-workers [27] used silver-coated zeolite crystals as SERS substrates while Wei et al. [28] find Ag films to be more Raman active than clusters or nanocrystals. Chaney et al. [29] found SERS activity of Ag nanorod arrays to depend on the length of the rods. Reproducibility of SERS

signals from place to place on films is generally not satisfactory. Atomic layer deposition and template electrodeposition have been employed to obtain uniform and reproducible SERS signals from films [30,31]. Wang and co-workers [32] have studied the effect of the morphology of Au films on the SERS signal. Bimetallic Au–Ag structures have also been employed as SERS substrates [33,34].

Since films are desirable substrates for SERS, we considered it important to investigate SERS activity of molecules on nanocrystalline films of Au and Ag which can be readily prepared at the organic–aqueous interface [35–37]. This technique of preparing film substrates is simple and involves generating the metallic films at the interface by the reaction of a metal precursor in the organic phase with a reducing agent in the aqueous phase. The films so-prepared contain nanoparticles of Au or Ag whose diameter can be varied by varying the temperature. Reaction parameters such as temperature, reaction time, concentrations of the metal precursor and the reducing agent, and the viscosity of the aqueous layer affect the nature and properties of the nanocrystalline films [36,37]. An additional advantage of the films generated at the interface is that they are easily transferred onto solid substrates. In this article, we present the results of our investigations of SERS of pyridine and rhodamine 6G on ultrathin nanocrystalline metallic films formed at the organic–aqueous interface.

2. Experimental

Nanocrystalline films of gold were prepared using $\text{Au}(\text{PPh}_3)\text{Cl}$ (Ph = phenyl) and $\text{Ag}(\text{PPh}_3)_4\text{NO}_3$ as precursors by the literature procedure [38,39]. Tetrakis(hydroxymethyl)phosphonium chloride (THPC) was used as the reducing agent. In a typical preparation, 10 mL of a 1.5 mM solution of $\text{Au}(\text{PPh}_3)\text{Cl}$ in toluene was allowed

* Corresponding author. Address: Chemistry and Physics of Materials Unit, New Chemistry Unit, and CSIR Centre of Excellence in Chemistry, Jawaharlal Nehru Centre for Advanced Scientific Research, Jakkur P.O., Bangalore 560 064, India. Fax: +91 80 2208 2766.

E-mail address: cnrrao@jncasr.ac.in (C.N.R. Rao).

to stand in contact with 16 mL of 6.25 mM aqueous alkali in a 100 mL beaker at room temperature. Once the two layers stabilized, 330 μ L of 50 mM THPC solution in water was injected into the aqueous layer using a syringe with minimal disturbance to the toluene layer. The onset of reduction was marked by a faint pink coloration of the toluene–water interface. The reduction was allowed to proceed without disturbance for a few hours. With the passage of time, the color became more vivid, finally resulting in a robust elastic film at the liquid–liquid interface [35]. To vary the particle size, the films were formed at different temperatures. Films of Ag were prepared by a similar procedure [35]. Nanocrystalline films of gold were also prepared by using hydrazine hydrate (50 μ L in 20 mL water) as the reducing agent, maintaining the temperature at 323 K. Au–Ag alloy films were prepared using the procedure reported in the literature [40]. Alloy formation was confirmed by changes in the visible spectra wherein the plasmon band shifts with the composition. 1:1 ratio of metal precursors (1.5 mM) in 10 mL toluene formed the organic layer and 16 mL 6.25 mM NaOH formed lower aqueous layer. 330 μ L 50 mM THPC was used as reducing agent, and the temperature maintained at 348 K. The nanocrystalline films were characterized by transmission electron microscopy (TEM) and other techniques. The thickness of the films was generally around 60 nm. Properties of the films were entirely reproducible, provided the conditions of preparation were kept the same.

For SERS measurements, we used pyridine and rhodamine 6G (Rh6G) solutions in water. For each measurement 10 μ L of the liquid analyte was dropped on nanocrystalline metallic film on a silicon wafer. Raman spectra were recorded with a LabRAM HR high-resolution Raman spectrometer (Horiba-Jobin Yvon) using a He–Ne laser ($\lambda = 632.8$ or 514 nm). We have obtained relative

enhancement ratios (R) of the adsorbate bands relative to those of the pure liquid [25,41,42] and have estimated the values of surface enhancement factor (EF). The relative enhancement ratio, R , is defined as the relative intensity of the Raman band of liquid analyte adsorbed on the nanocrystalline film divided by the relative intensity of corresponding band of liquid pyridine or Rh6G solution. The surface enhancement factor, EF, was calculated by the equation [3,19],

$$EF = (I_{\text{SERS}}/I_{\text{bulk}})(N_{\text{bulk}}/N_{\text{ads}})$$

where I_{SERS} , I_{bulk} , N_{bulk} and N_{ads} respectively represent the measured SERS intensity of adsorbed molecules on the Au/Ag nanocrystalline film, the normal Raman intensity from the liquid analyte, the number of probe molecules under laser illumination in the bulk sample, and the number of probe molecules on the nanocrystalline film respectively. N_{ads} is calculated from the average radius of adsorbate nanoparticles, the surface density of the adsorbate molecule, the area of the laser spot, and surface coverage of adsorbate nanoparticles. N_{bulk} was obtained from the area of the laser spot, the penetration depth, the density of the analyte, and the molecular weight of the analyte. SERS measurements were made on different places of a given sample to ensure reproducibility of the results.

3. Results and discussion

We first carried out SERS of pyridine on nanocrystalline Au films generated at the liquid–liquid interface by using THPC as the reducing agent. In Fig. 1a–c, we show TEM images of the Au nanocrystalline films formed at different temperatures. The Au particles in the films formed at 298, 313 and 348 K had average diameters of 10, 12 and 15 nm respectively. Fig. 2A shows the Raman spectra of

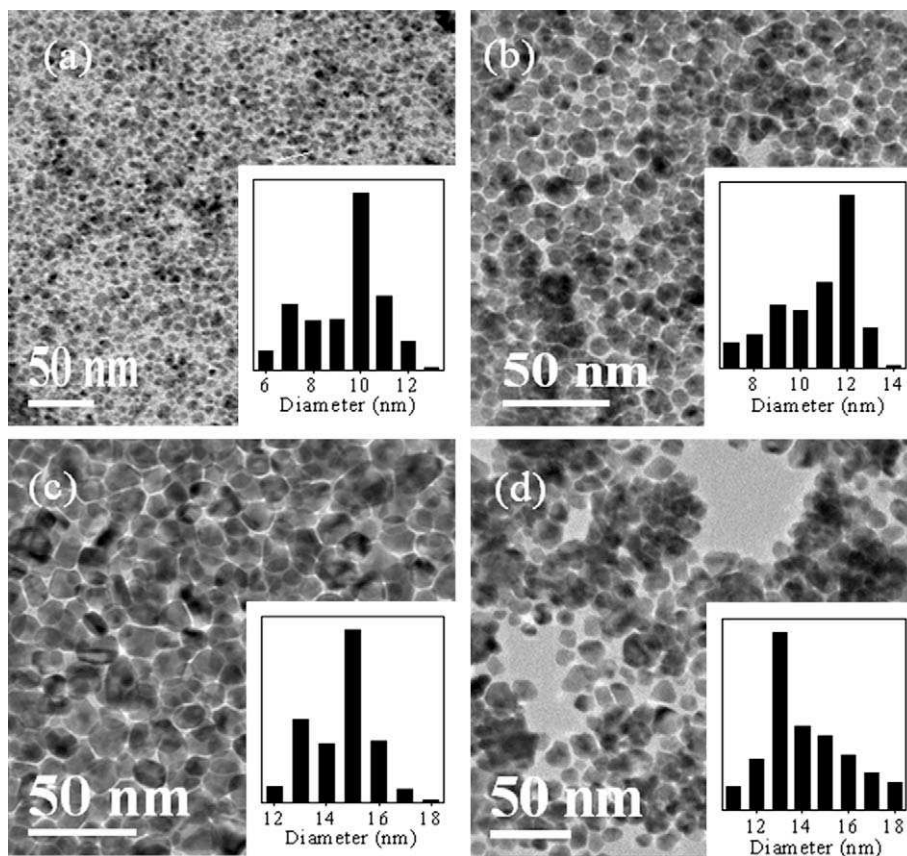


Fig. 1. TEM images of the ultrathin nanocrystalline Au films obtained at the liquid–liquid interface using THPC as the reducing agent at (a) 298 K, (b) 313 K, (c) 348 K and of (d) with hydrazine hydrate as the reducing agent at 323 K. Histograms of particle size distribution are shown as insets.

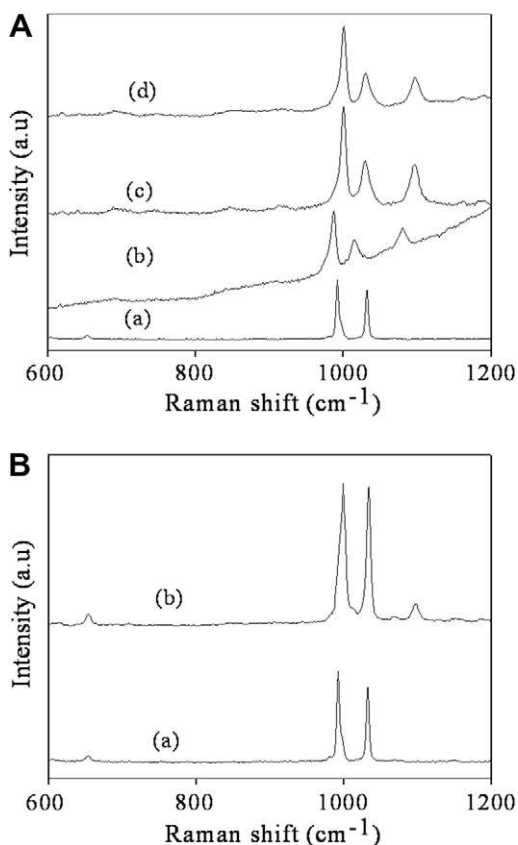


Fig. 2. (A) Raman spectra of pyridine ($\lambda = 632$ nm) (a) in the liquid state and on Au films with particles of diameter (b) 10, (c) 12 and (d) 15 nm prepared at toluene-water interface using THPC as the reducing agent. (B) Raman spectra of pyridine (a) in liquid state and (b) on 13 nm ultrathin nanocrystalline Au film prepared using hydrazine hydrate as the reducing agent ($\lambda = 632$ nm).

pyridine on the Au nanocrystalline films containing particles of different diameters, along with the spectrum of the pure liquid. We clearly see SERS on the Au films. Thus, on adsorption of pyridine on the Au film containing particles of 15 nm diameter, we observe bands at 619 cm^{-1} (ν_{6a} , A_1 , asymmetric ring breathing), 689 cm^{-1} (ν_{6b} , B_2 , ring in plane deformation), 1001 cm^{-1} (ν_1 , A_1 , symmetric ring breathing), 1030 cm^{-1} (ν_{12} , A_1 , trigonal ring breathing), 1096 cm^{-1} (ν_{18a} , A_1) and 1298 cm^{-1} (ν_{9a} , A_1 , C–H in plane deformation) respectively. In Table 1, we compare the Raman band positions of pyridine on Au nanocrystalline films with different particle diameters along with their relative intensities. We see that almost all the bands are shifted to higher frequencies (relative to the positions of the pure liquid), except those at 1032, 1441 and 1482 cm^{-1} . The highest frequency shifts are exhibited by the bands at 652 cm^{-1} (ν_{6b} , B_2) and 1068 cm^{-1} (ν_{18a} , A_1). The highest intensity is found in the case of the symmetric ring breathing mode (ν_1) at 1001 cm^{-1} . The frequency of this mode is sensitive to weak σ donation and the large σ/π back donation. In the case of Au and other metals, the ν_1 mode is known to be shifted to higher frequencies, with the pyridine molecule in the end-on configuration (binding by nitrogen lone pair) [16,25]. That we observe similar shifts of ν_1 in the present study, on adsorbing pyridine on the Au nanocrystalline films, suggests the end-on configuration for the adsorbed molecule. We also observe additional bands around 1190 and 1185 cm^{-1} .

We have measured the relative enhancement ratios, R , of pyridine on the Au nanocrystalline films and found that it to vary between 1.0 and 22, depending on the particle size (Table 1), the maximum values of R being found with the 12 nm particles. The

Table 1

Raman band positions (cm^{-1}) and relative enhancement ratios of pyridine on nanocrystalline Au films.

Liquid peak positions (relative intensity)	ν	Films of 12 nm Au ^a		Films of 15 nm Au ^a		Films of 13 nm Au ^b	
		Peak positions (relative intensity)	R	Peak positions (relative intensity)	R	Peak positions (relative intensity)	R
604, A_1 (2)	6a	620 (3)	2	619 (4)	2	616 (1.5)	0.75
652, B_2 (5)	6b	689 (7)	1	689 (5)	1	653 (9)	2.0
992, A_1 (100)	1	1000 (100)	1	1001 (100)	1	999 (100)	1
1032, A_1 (82)	12	1029 (42)	0.5	1030 (41)	0.5	1033 (98)	1.2
1068, A_1 (2)	18a	1097 (43)	22	1096 (33)	17	1096 (11.5)	6.0
1149, B_2 (2)	15	1163 (4)	2	1161 (5)	3	1152 (3)	1.5
		1191 (4)		1190 (4)		1185 (2)	
1218, A_1 (7)	9a			1298 (5)	0.7	1218 (8)	1
1441, B_2 (1)	19b	1437 (5)	5	1440 (3)	3	1436 (3)	3
1482, A_1 (2)	19a	1480 (3)	2	1483 (1)	0.5	1485 (2)	1
1573, B_2 (2)	8b	1572 (3)	2			1575 (9)	4.5
1583, A_1 (2)	8a	1585 (21)	11	1585 (56)	28	1584 (11)	5.5

ν = Wilson number; R = relative enhancement ratio.

^a By THPC route.

^b By hydrazine hydrate route.

SERS intensity is optimal when the particle size is small with respect to the wavelength of the exciting light as long as the size is not smaller than the electronic mean free path of the conduction electrons. In order to calculate EF, we have used the value of monolayer surface density of pyridine [16] on Au as $4 \times 10^{-10}\text{ mol cm}^{-2}$. We have calculated EF values for the three most intense bands in liquid pyridine spectra: ν_1 (992 cm^{-1} , A_1), ν_{12} (1032 cm^{-1} , A_1) and ν_{18a} (1068 cm^{-1} , A_1). The EF values listed in Table 2 show that they are generally of the order of $\sim 10^5$ and comparable to those reported in other SERS studies [3].

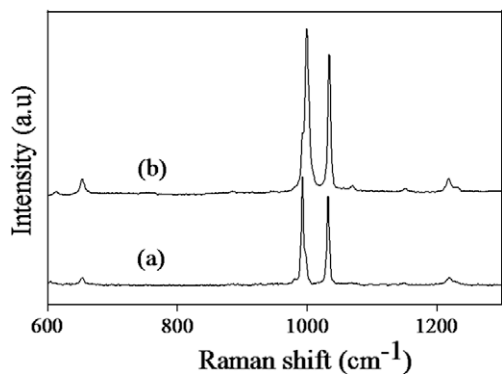
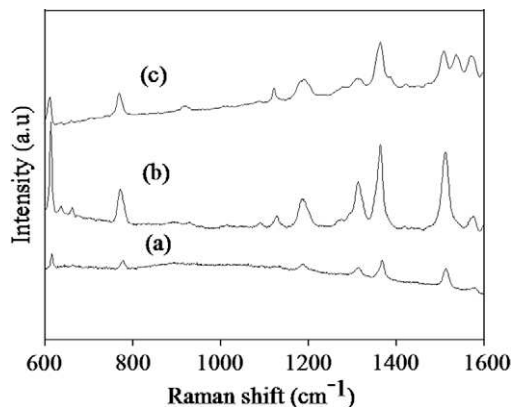
TEM images of Au films formed at 323 K with hydrazine hydrate as the reducing agent show that the nanocrystals had an average diameter of 13 nm (Fig. 1d). The Raman spectrum of pyridine on this nanocrystalline film is shown along with spectrum of pure pyridine in Fig. 2B. We find the shifts and intensification of the pyridine bands on this Au film to be similar to those found with the films prepared with THPC (see Table 1). The R values of the pyridine bands vary in range 1–6.

We have measured SERS activity of pyridine on Ag nanocrystalline films formed at the liquid–liquid interface at 348 K and containing particles with an average diameter of around 35 nm. All the Raman bands of pyridine show shifts to higher frequencies on the Ag film (Fig. 3), but the shifts are less than those on Au films. The value of R varies between 1 and 3 while EF is 6.5×10^4 , 6.7×10^4 and 7.0×10^4 for the ν_1 (992 cm^{-1} , A_1), ν_{12} (1032 cm^{-1}) and ν_{18a} (1068 cm^{-1} , A_1) modes respectively. The intensity of the ν_{12} band gets enhanced much more on the Ag film than on the Au films. It is known that the potential energy distribution of the ν_{12} mode varies substantially for metals with different Fermi levels [3]. Unlike on the Au films where few of the pyridine bands show intensification, all the bands of pyridine show intensification in the case Ag, suggesting that EM enhancement plays a more important role and that chemical interaction between pyridine and Ag is relatively weak [3,43]. In the case of Au films, however, both EM and chemical enhancements occur. Measurements of SERS of pyridine with films comprising nanoparticles of the 1:1 alloy of Au–Ag show R values comparable to those on Au and Ag films.

SERS activity of rhodamine 6G was investigated on the 35 nm Ag film, by recording the spectra with both 632 and 514 nm laser excitations, since the dye shows strong fluorescence with an absorbance maximum at 520 nm. Fig. 4 shows the Raman spectra of 10^{-2} M rhodamine 6G (in water) adsorbed on the Ag film using

Table 2Selected Raman band positions (cm^{-1}) and enhancement factors (EF) of pyridine on nanocrystalline Au films.

Liquid peak positions (relative intensity)	ν	Films of 12 nm Au ^a		Films of 15 nm Au ^a		Films of 13 nm Au ^b	
		Peak positions (relative intensity)	EF	Peak positions (relative intensity)	EF	Peak positions (relative intensity)	EF
992, A ₁ (100)	1	1000 (100)	2.3×10^4	1001 (100)	4.0×10^4	999 (100)	3.3×10^3
1032, A ₁ (82)	12	1029 (42)	1.2×10^4	1030 (41)	2.0×10^4	1033 (98)	3.1×10^3
1068, A ₁ (2)	18a	1097 (43)	5.0×10^5	1096 (33)	6.0×10^5	1097 (11.5)	2.9×10^4

 ν = Wilson number; EF = enhancement factor.^a By THPC route.^b By hydrazine hydrate route.**Fig. 3.** Raman spectra of pyridine ($\lambda = 632$ nm) (a) in the liquid state, and (b) on a ultrathin nanocrystalline Ag film with 35 nm particles.**Fig. 4.** Raman spectra of rhodamine 6G (in water) (a) in the liquid state ($\lambda = 632$ nm) and on the nanocrystalline Ag film with λ of (b) 632 nm and (c) 514 nm.

both 632 nm and 514 nm laser excitations. The spectrum of the pure liquid is shown for comparison. On adsorption of rhodamine 6G on the Ag film, we observe a large number of bands, all shifted to lower frequencies [43]. We also observe additional bands at 636, 1270, 1293 and 1476 cm^{-1} . The two most intense bands of rhodamine 6G 1367 cm^{-1} [$\nu(\text{CC}) + \nu(\text{CN})$] and 1515 cm^{-1} [$\nu(\text{CC})$] are shifted to 1363 and 1512 cm^{-1} respectively on adsorption on the Ag film. The R values of rhodamine 6G on Ag vary between 1.0 and 1.4. The EF values for the four most intense bands of rhodamine 6G ν_{53} at 615 cm^{-1} , ν_{115} at 1314 cm^{-1} , ν_{117} at 1367 cm^{-1} and ν_{146} at 1515 cm^{-1} was found to be of the order of 10^4 .

4. Conclusions

The results of the present study show that nanocrystalline films of Au and Ag generated at the organic–aqueous interface can be

used as substrates for SERS studies of molecules. The intensity enhancement and band shifts of pyridine found on these thin films are comparable to those reported for other Au and Ag substrates. The ease with which nanocrystalline metal films are prepared at the interface favor their use for SERS studies.

References

- [1] M. Fleischmann, P.J. Hendra, A.J. McQuillan, Chem. Phys. Lett. 26 (1974) 163.
- [2] R.K. Chang, T.E. Furtak, Surface Enhanced Raman Scattering, New York, Plenum Press, 1982.
- [3] Z.Q. Tian, B. Ren, D.Y. Wu, J. Phys. Chem. B 106 (2002) 9463.
- [4] M.J. Moskovits, Raman Spectrosc. 36 (2005) 485.
- [5] K. Kneipp, H. Kneipp, I. Itzkan, R.R. Dasari, M.S. Feld, Chem. Rev. 99 (1999) 1957.
- [6] C.J. Orendorff, A. Gole, T.K. Sau, C.J. Murphy, Anal. Chem. 77 (2005) 3261.
- [7] A. Campion, P. Kambhampati, Chem. Soc. Rev. 27 (1998) 241.
- [8] C. Lee, S.J. Bae, M. Gong, K. Kim, S.W. Joo, J. Raman Spectrosc. 33 (2002) 429.
- [9] C.J. Orendorff, L. Gearheart, N.R. Jana, C.J. Murphy, Phys. Chem. Chem. Phys. 8 (2006) 165.
- [10] M. Kerker, Pure Appl. Chem. 56 (1984) 1429.
- [11] R. Dornhaus, M.B. Long, R.E. Benner, R.K. Chang, Surf. Sci. 93 (1980) 240.
- [12] M.M. Miranda, N. Neto, G. Sbrana, J. Phys. Chem. 92 (1988) 954.
- [13] H.H. Wang et al., Adv. Mater. 18 (2006) 491.
- [14] A.M. Michaels, M. Nirmal, L.E. Brus, J. Am. Chem. Soc. 121 (1999) 9932.
- [15] K.A.B. Snick, J. Jiang, L.E. Brus, J. Phys. Chem. B 106 (2002) 8096.
- [16] A.G. Brolo, D.E. Irish, J. Lipkowski, J. Phys. Chem. B 101 (1997) 3906.
- [17] N. Felidj et al., J. Chem. Phys. 120 (2004) 7141.
- [18] X.C. Yang, Y. Fang, J. Phys. Chem. B 107 (2003) 10100.
- [19] Z. Zhu, T. Zhu, Z. Liu, Nanotechnology 15 (2004) 357.
- [20] B. Ren, Q.J. Huang, W.B. Chai, B.W. Mao, F.M. Liu, Z.Q. Tian, J. Electroanal. Chem. 415 (1996) 175.
- [21] J.S. Gao, Z.Q. Tian, Spectrochim. Acta A 53 (1997) 1595.
- [22] Q.J. Huang, J.L. Yao, R.A. Gu, Z.Q. Tian, Chem. Phys. Lett. 271 (1997) 101.
- [23] P.G. Cao, J.L. Yao, B. Ren, B.W. Mao, R.A. Gu, Z.Q. Tian, Chem. Phys. Lett. 316 (2000) 1.
- [24] D.Y. Wu, Y. Xie, B. Ren, J.W. Yan, B.W. Mao, Z.Q. Tian, Phys. Chem. Commun. 18 (2001) 1.
- [25] C. Zou, P.W. Jagodzinski, J. Phys. Chem. B 109 (2005) 1788.
- [26] K. Biswas, S.V. Bhat, C.N.R. Rao, J. Phys. Chem. C 111 (2007) 5689.
- [27] W. Yan, L. Bao, S.M. Mahurin, S. Dai, Appl. Spectrosc. 58 (2006) 18.
- [28] G. Wei, H. Zhou, Z. Liu, Z. Li, Appl. Surf. Sci. 240 (2005) 260.
- [29] S.B. Chaney, S. Shanmukh, R.A. Dluhý, Y.P. Zhao, Appl. Phys. Lett. 87 (2005) 031908.
- [30] J.A. Dieringer et al., Faraday Discuss. 132 (2006) 9.
- [31] M.E. Abdelsalam, P.N. Bartlett, J.J. Baumberg, S. Cintra, T.A. Kelf, A.E. Russell, Electrochem. Commun. 7 (2005) 740.
- [32] C.H. Wang, D.C. Sun, X.H. Xia, Nanotechnology 17 (2006) 651.
- [33] S.E. Hunyadi, C.J. Murphy, J. Mater. Chem. 16 (2006) 3929.
- [34] Y. Wang, H. Chen, H. Dong, E. Wang, J. Chem. Phys. 125 (2006) 044710.
- [35] C.N.R. Rao, G.U. Kulkarni, P.J. Thomas, V.V. Agrawal, P. Saravanan, J. Phys. Chem. B 107 (2003) 7391.
- [36] C.N.R. Rao, G.U. Kulkarni, V.V. Agrawal, U.K. Gautam, M. Ghosh, U. Tumkurkar, J. Colloid Interface Sci. 289 (2005) 305.
- [37] C.N.R. Rao, K.P. Kalyanikutty, Acc. Chem. Res. 41 (2008) 489.
- [38] P. Braunstein, H. Lehner, D. Matt, Inorg. Synth. 7 (1990) 218.
- [39] M. Khan, C. Oldham, D.G. Tuck, Can. J. Chem. 59 (1981) 2714.
- [40] V.V. Agrawal, P. Mahalakshmi, G.U. Kulkarni, C.N.R. Rao, Langmuir 22 (2006) 1846.
- [41] S. Astilean, M. Bolboaca, D. Mainu, T. Iliescu, Romanian Rep. Phys. 56 (2004) 346.
- [42] P. Hildebrandt, M. Stockburger, J. Phys. Chem. 88 (1984) 5935.
- [43] H. Watanabe, N. Hayazawa, Y. Inouye, S. Kawata, J. Phys. Chem. B 109 (2005) 5012.